Scientific Report

TRANSPARENT PROCESS

EMBO reports

53BP1 ablation rescues genomic instability in mice expressing 'RING-less' BRCA1

Minxing Li[1], Francesca Cole[2,3], Dharm S Patel[1], Sarah M Misenko[1], Joonyoung Her[1], Amy Malhowski[4], Ali Alhamza[1], Haiyan Zheng[5], Richard Baer[6], Thomas Ludwig[7], Maria Jasin[2], André Nussenzweig[4], Lourdes Serrano[8] & Samuel F Bunting[1,*]

Abstract

***BRCA1* mutations strongly predispose affected individuals to breast and ovarian cancer, but the mechanism by which BRCA1 acts as a tumor suppressor is not fully understood. Homozygous deletion of exon 2 of the mouse *Brca1* gene normally causes embryonic lethality, but we show that exon 2-deleted alleles of *Brca1* are expressed as a mutant isoform that lacks the N-terminal RING domain. This "RING-less" BRCA1 protein is stable and efficiently recruited to the sites of DNA damage. Surprisingly, robust RAD51 foci form in cells expressing RING-less BRCA1 in response to DNA damage, but the cells nonetheless display the substantial genomic instability. Genomic instability can be rescued by the deletion of *Trp53bp1*, which encodes the DNA damage response factor 53BP1, and mice expressing RING-less BRCA1 do not show an increased susceptibility to tumors in the absence of 53BP1. Genomic instability in cells expressing RING-less BRCA1 correlates with the loss of BARD1 and a defect in restart of replication forks after hydroxyurea treatment, suggesting a role of BRCA1–BARD1 in genomic integrity that is independent of RAD51 loading.**

Keywords cancer; DNA repair; genomic integrity; mouse models; RAD51
Subject Category DNA Replication, Repair & Recombination
DOI 10.15252/embr.201642497 | Received 5 April 2016 | Revised 8 September 2016 | Accepted 9 September 2016 | Published online 26 September 2016
EMBO Reports (2016) 17: 1532–1541

Introduction

Mutations in the *BRCA1* gene account for approximately 7% of human hereditary breast and ovarian cancer cases, and mutation of the *Brca1* gene also causes cancer in mice [1,2]. Despite the importance of *BRCA1* mutations in human disease, the precise mechanism by which BRCA1 mediates DNA repair is still unclear. Cells lacking functional BRCA1 often show a defect in the homologous recombination (HR) pathway for the repair of DNA double-strand breaks (DSBs) [2,3]. This defect leads to genomic instability in *BRCA1*-deficient cells and contributes to tumorigenesis.

Recent research efforts have aimed to determine which of the conserved domains within the BRCA1 protein are most important for its activity. The N-terminal RING domain forms a heterodimer with BRCA1-Associated RING Domain protein 1 (BARD1) that acts as an E3 ubiquitin ligase [4–6]. E3 ligase activity of BRCA1–BARD1 may contribute to genomic integrity by ubiquitylating chromatin at repetitive satellite DNA elements, which keeps these regions in a transcriptionally silent state [7]. Other mouse models have, however, shown that the inactivation of BRCA1's ability to act as an E3 ubiquitin ligase has a negligible effect on tumor suppressor activity and that the C-terminal BRCT domains are of greater importance [8,9]. A new perspective on BRCA1's cellular function has come from the finding that targeting of the DNA damage response factor 53BP1 rescues many of the phenotypes associated with BRCA1 deficiency. Mice carrying homozygous mutations in *Brca1* are normally not viable, but deletion of *Trp53bp1*, which encodes 53BP1, rescues embryonic lethality [10]. Ablation of 53BP1 has been shown to normalize the rates of HR in *Brca1*-deficient cells [11,12], suggesting that 53BP1 may act to limit the use of the HR pathway for DSB repair. It is not known how BRCA1 counteracts this inhibitory effect of 53BP1 on HR.

To better understand how BRCA1 and 53BP1 regulate mammalian double-strand break repair, we studied two mouse models of *Brca1* deficiency featuring replacement or the deletion of *Brca1* exon 2. These are $Brca1^{ex2/ex2}$ mice, in which exon 2 is replaced by a *neo* cassette, and $Brca1^{\Delta 2/\Delta 2}$ mice, in which exon 2 is conditionally deleted by *Cre-loxP* recombination [13,14]. We find that both of these strains express a mutant BRCA1 protein isoform that lacks the N-terminal RING domain. This mutant BRCA1 isoform

1 Department of Molecular Biology and Biochemistry, Rutgers, The State University of New Jersey, Piscataway, NJ, USA
2 Developmental Biology Program, Memorial Sloan-Kettering Cancer Center, New York, NY, USA
3 Department of Epigenetics and Molecular Carcinogenesis, The University of Texas MD Anderson Cancer Center, Smithville, TX, USA
4 Laboratory of Genome Integrity, Center for Cancer Research, National Cancer Institute, National Institutes of Health, Bethesda, MD, USA
5 Biological Mass Spectrometry Facility, Rutgers, The State University of New Jersey, Piscataway, NJ, USA
6 Institute of Cancer Genetics, Department of Pathology & Cell Biology, Columbia University Medical Center, New York, NY, USA
7 Department of Cancer Biology & Genetics, Ohio State University, Columbus, OH, USA
8 Department of Genetics, Human Genetics Institute of New Jersey, Rutgers, The State University of New Jersey, Piscataway, NJ, USA
*Corresponding author. Tel: +1 848 445 9894; E-mail: bunting@cabm.rutgers.edu

can support the accumulation of RAD51 at sites of DNA damage, although cells expressing the mutant isoform nonetheless show genomic instability and a defect in replication fork stability. These findings suggest that the RING domain of BRCA1 plays an essential role in replication fork stability that is independent of RAD51 foci formation.

Results and Discussion

Homozygous *Brca1*$^{ex2/ex2}$ mice show embryonic lethality at an early stage of development [13]. The start codon for translation of the full-length BRCA1 polypeptide, which is encoded in exon 2, is deleted in the *Brca1*^{ex2} allele (Fig 1A). The *Brca1*^{ex2} allele has therefore been considered to be a "null" allele of *Brca1* [15]. The early embryonic lethality of *Brca1*$^{ex2/ex2}$ mice can, however, be rescued by codeletion of *Trp53bp1*, which encodes the DNA repair factor, 53BP1 [16]. We prepared *Brca1*$^{ex2/ex2}$;*Trp53bp1*$^{-/-}$ mouse embryonic fibroblasts (MEFs) and found that these cells produce a *Brca1* transcript in which exon 1 is spliced directly to exon 3 (Fig 1A). This *Brca1* transcript contains all known protein-coding exons after exon 3 and is translated to make a BRCA1 isoform that is slightly smaller than the full-length ~220-kDa protein (Fig 1B). Mass spectrometry showed that the start site for translation of the mutant protein is either Met-90 or Met-99 (which lie within the same tryptic fragment). Translation starting at either of these sites would be in the correct frame to produce a ~210-kDa BRCA1 polypeptide, consistent with our Western blot results. The absence of the N-terminal region means that almost all of the RING domain, which is made up of residues 1–109 in the WT protein [17], is missing from the mutant protein isoform. Instead of a null allele, *Brca1*^{ex2} is therefore expressed as a "RING-less" form of BRCA1.

BRCA1 and BARD1 form a heterodimer through the contacts made between their respective RING domains, and heterodimerization normally stabilizes both proteins [6,17,18]. In *Brca1*$^{ex2/ex2}$;*Trp53bp1*$^{-/-}$ cells, which express RING-less BRCA1, there is no detectable BARD1 protein (Fig 1B). In contrast, *Brca1*$^{\Delta 11/\Delta 11}$;*Trp53bp1*$^{-/-}$cells, which express a mutant BRCA1 isoform with an intact RING domain (BRCA1$^{\Delta 11}$), showed no reduction in BARD1. RING-less BRCA1 appears stable, presumably because the N-terminal degron normally found within amino acids 1–167 is deleted [19]. Although it cannot form a heterodimer with BARD1, robust nuclear foci of BRCA1 protein were observed in both WT and *Brca1*$^{ex2/ex2}$;*Trp53bp1*$^{-/-}$ cells in response to ionizing radiation (IR). These BRCA1 foci showed colocalization with RAD51 at DNA damage sites equivalent to that seen in WT cells (Fig 1C–E). Conversely, nuclear foci of BARD1 were absent in *Brca1*$^{ex2/ex2}$;*Trp53bp1*$^{-/-}$ cells (Fig 1F), consistent with the very low level of stable BARD1.

To test the activity of RING-less BRCA1, we used mice carrying the conditional *Brca1*^{flex2} allele, in which *Brca1* exon 2 can be deleted by the expression of Cre recombinase. A previous study using these mice showed that conditional deletion of exon 2 in the mammary epithelium leads to tumor formation [14]. As was the case with the *Brca1*^{ex2} allele, *Brca1* exon 2-deleted cells (*Brca1*$^{\Delta 2/\Delta 2}$) express a variant ~210-kDa protein product derived from splicing of exon 1 directly to exon 3 (Fig 2A). Levels of BARD1 are also substantially reduced in *Brca1*$^{\Delta 2/\Delta 2}$ cells, consistent with a failure of the mutant, RING-less BRCA1 isoform to stabilize BARD1 protein. The BRCA1$^{\Delta 2}$ protein is expressed in both *Trp53bp1*$^{-/-}$ and *Trp53bp1*$^{+/+}$ cells (Fig EV1A), allowing us to study the activity of RING-less BRCA1 in cells that express 53BP1 (henceforth "*Brca1*$^{\Delta 2/2\Delta 2}$"). *Brca1*$^{\Delta 2/\Delta 2}$ B cells showed elevated rates of spontaneous chromosome aberrations and especially high rates of genomic instability after treatment with the poly (ADP-ribose) polymerase inhibitor, olaparib, which increases the frequency of DNA DSBs (Fig 2B). Hypersensitivity was also observed in *Brca1*$^{\Delta 2/\Delta 2}$ cells exposed to cisplatin, which covalently crosslinks DNA and impedes replication (Fig EV1B).

Surprisingly, genomic instability in *Brca1*$^{\Delta 2/\Delta 2}$ cells did not correlate with a failure to form irradiation-induced nuclear RAD51 foci, as is typically seen in other models of *Brca1* deficiency such as *Brca1*$^{\Delta 11}$ or *Brca1*$^{\Delta 5-13}$ (Fig 2C) [11,12]. *Brca1*$^{\Delta 2/\Delta 2}$ cells formed IR-induced RAD51 foci at an equivalent rate to that observed in WT cells, and also formed robust RAD51 foci after treatment with olaparib or camptothecin (Fig 2D). BRCA1 normally forms a ternary complex at break sites with PALB2 (Partner and Localizer of BRCA2) and BRCA2, which helps load RAD51 onto resected DNA ends [20]. BRCA1 binds PALB2 through the association of coiled coil motifs in both proteins [21]. The BRCA1 coiled coil motif is still present in RING-less BRCA1, potentially explaining why the mutant protein is able to support RAD51 foci formation after DNA damage. Ionizing radiation-induced γ-H2AX foci were also resolved with equivalent kinetics in WT and *Brca1*$^{\Delta 2/\Delta 2}$ cells (Fig 2E), indicating that there is no overt defect in DSB repair in cells expressing RING-less BRCA1. Finally, we tested the efficiency of homologous recombination in *Brca1*$^{\Delta 2/\Delta 2}$ cells by measuring the frequency of sister chromatid exchanges (SCEs), which are formed by crossover recombination during repair of DSBs. No reduction in the frequency of spontaneous or olaparib-induced SCEs was observed between WT and *Brca1*$^{\Delta 2/\Delta 2}$ cells (Fig 2F). Taken together, these results suggest that genomic instability in cells expressing RING-less BRCA1 is not a consequence of deficient repair of DNA double-strand breaks.

In addition to a role in mediating RAD51 assembly at DSBs, BRCA1 has been implicated in the protection of newly synthesized DNA at stalled replication forks [22]. We therefore tested the stability of replication forks in *Brca1*$^{\Delta 2/\Delta 2}$ cells. We used a DNA combing assay to monitor fork progression after treatment with hydroxyurea (HU), which causes fork stalling (Fig 3A). The majority of replication tracts showed restart after HU was removed, as indicated by contiguous tracts of CldU and IdU staining. In the *Brca1*$^{\Delta 2/\Delta 2}$ cells, however, there was an elevated frequency of tracts that stained for CldU only, consistent with failure to restart the replication fork after HU-induced stalling (Fig 3B). RING-less BRCA1 therefore appears to be deficient in facilitating recovery from replication stress, which may account for the increased genomic instability in cells expressing this mutant isoform. We also examined the rate of activation of new origins, and the length of initial replication tracts, but found no substantial difference between WT and *Brca1*$^{\Delta 2/\Delta 2}$ cells (Fig 3C and D). Our results indicate that the RING domain of BRCA1, potentially in conjunction with BARD1, protects genomic integrity by enabling the restart of stalled replication forks. This role is distinct from BRCA1's role in mediating the assembly of RAD51 foci at DNA double-strand break sites, and is consistent with recent findings that protection of replication forks can rescue genome instability in BRCA-deficient cells without restoration of DSB repair via HR [23].

Ablation of 53BP1 rescues the embryonic lethality and genomic instability in mice carrying exon 2-deleted forms of *Brca1* (Fig 2B)

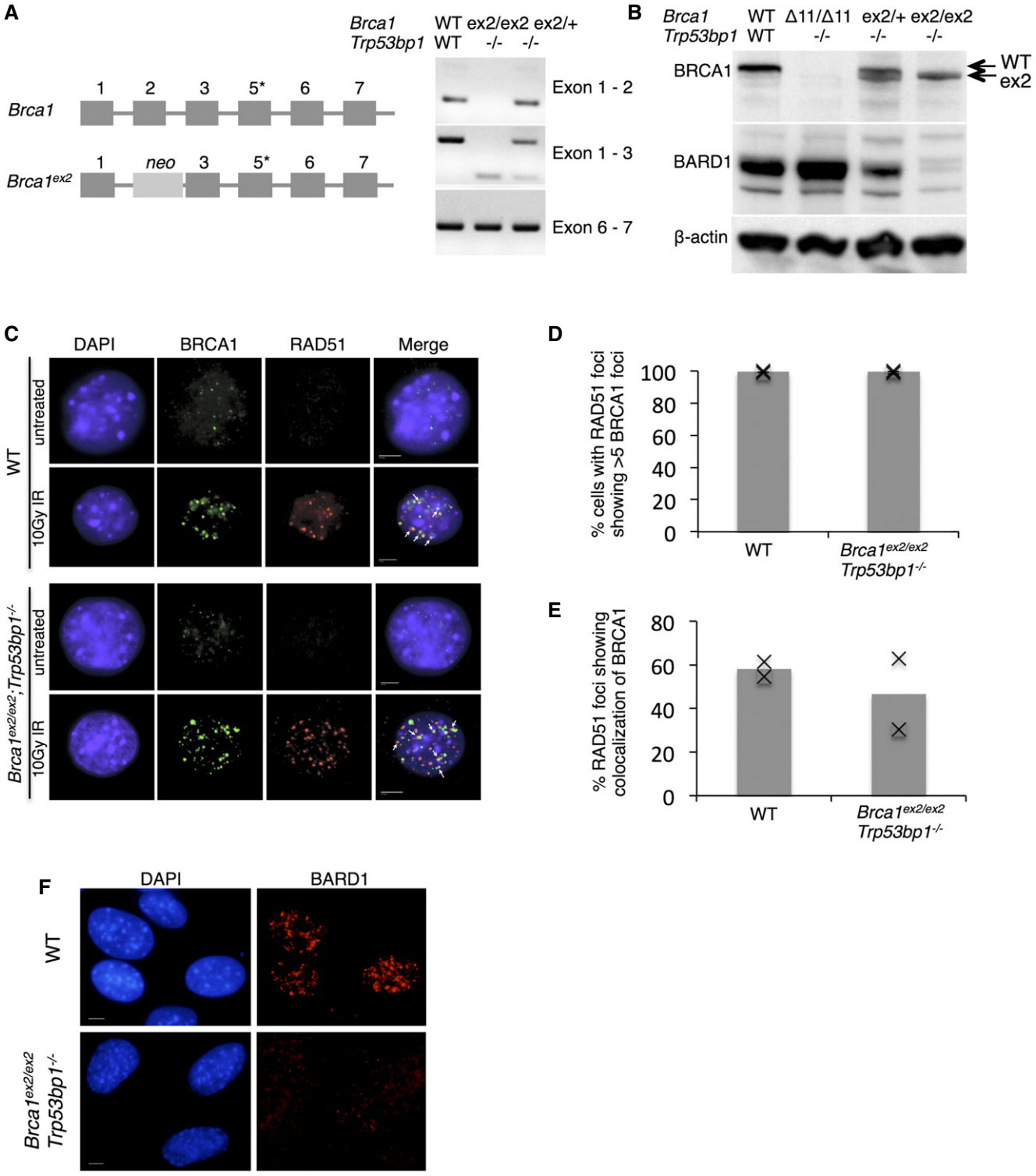

Figure 1. Targeting of *Brca1* exon 2 leads to production of a stable, N-terminal truncated protein isoform.

A Structure of *Brca1*^{ex2} allele. *Note that exon 4 was annotated in error in original descriptions of the gene structure and is not drawn. RT–PCR shows a novel product from the *Brca1*^{ex2} allele, corresponding to splicing of exon 1 directly to exon 3.

B Western blot to detect BRCA1 and BARD1 in MEFs expressing WT and mutant *Brca1*.

C Immunofluorescent (IF) detection of BRCA1 and RAD51 at IR-induced nuclear foci in cells expressing WT and mutant forms of *Brca1*. Scale bar: 10 μm.

D Quantification of IF, showing the proportion of cells with RAD51 foci that also had > 5 BRCA1 foci. $N = 2$.

E Quantification of IF, showing the proportion of RAD51 foci that colocalized with BRCA1 foci. $N = 2$.

F Immunofluorescent detection of BARD1 at IR-induced nuclear foci in MEFs expressing WT and mutant forms of *Brca1*. Scale bar: 10 μm.

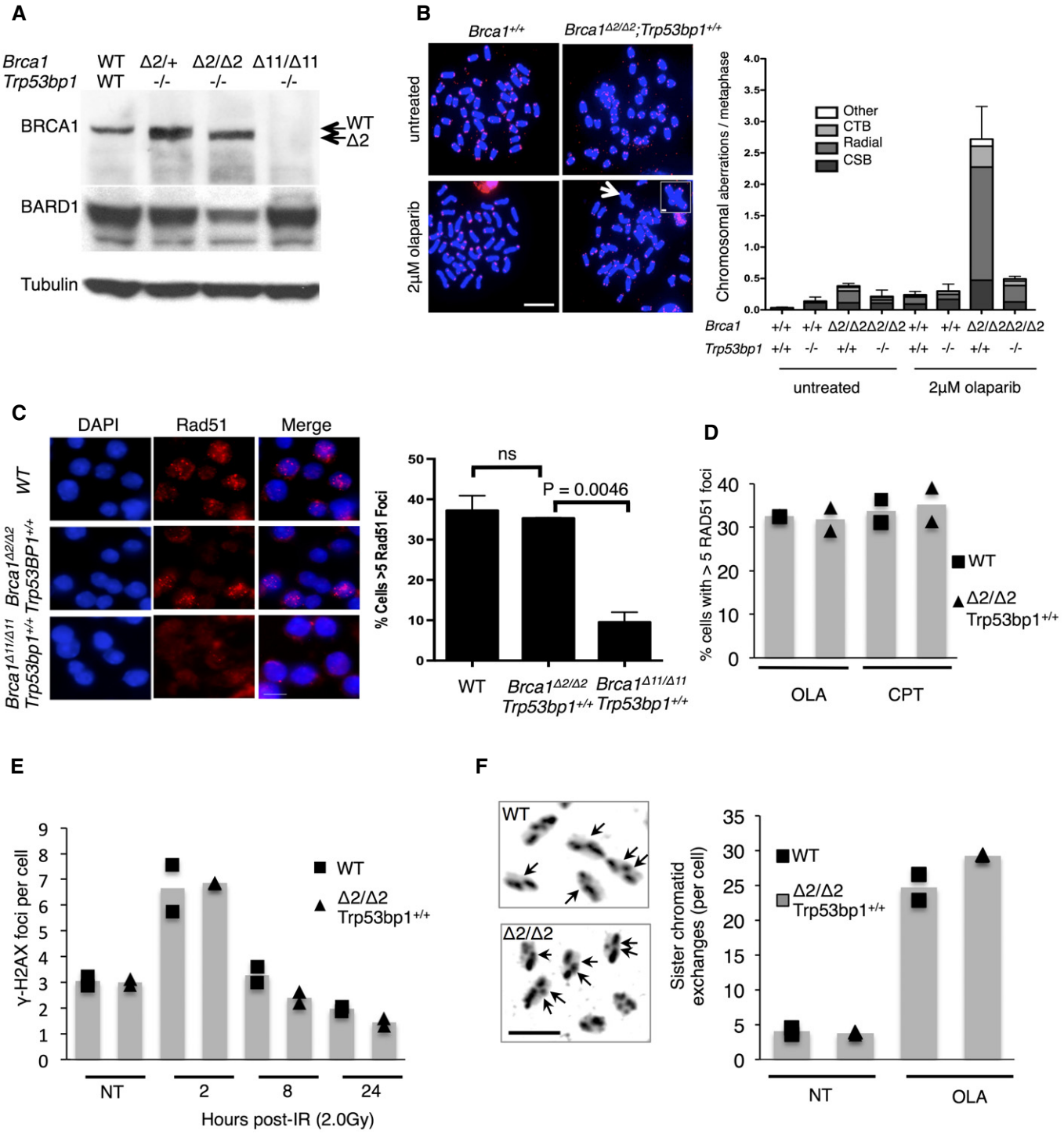

Figure 2. Conditional deletion of *Brca1* exon 2 causes genomic instability despite normal recruitment of RAD51 to DNA double-strand breaks.

A Western blot showing abundance of BRCA1 and BARD1 protein in *Brca1*$^{\Delta 2/\Delta 2}$;*Trp53bp1*$^{-/-}$ mouse B cells.

B Analysis of chromosome aberrations in mice with targeted deletion of *Brca1* exon 2 and *Trp53bp1*. Left, metaphase spreads were prepared from B cells treated with olaparib. Arrows show examples of chromosome aberrations. Right, quantification of chromosome breaks (CSB), chromatid-type breaks (CTD), radial chromosomes, and other abnormalities in mouse B cells. Error bars indicate SD, $N = 3$. Scale bar: 100 μm.

C RAD51 foci in B cells after 10 Gy IR exposure. Chart shows mean percentage of cells with > 5 foci, $N = 3$. Error bars indicate SD, statistical analysis by two-tailed Student's *t*-test. Scale bar: 10 μm.

D Percentage of cells showing > 5 RAD51 foci after 4-h treatment with 10 μM olaparib (OLA) or 10 μM camptothecin (CPT). $N = 2$.

E Average number of γ-H2AX foci per cell in cells that were not treated (NT) or exposed to 2 Gy ionizing radiation. $N = 2$.

F Sister chromatid exchanges in cells that were not treated (NT) or exposed to 2 μM olaparib (OLA) for 16 h. Black arrows in images show SCEs in olaparib-treated cells. Scale bar: 5 μm. $N = 2$.

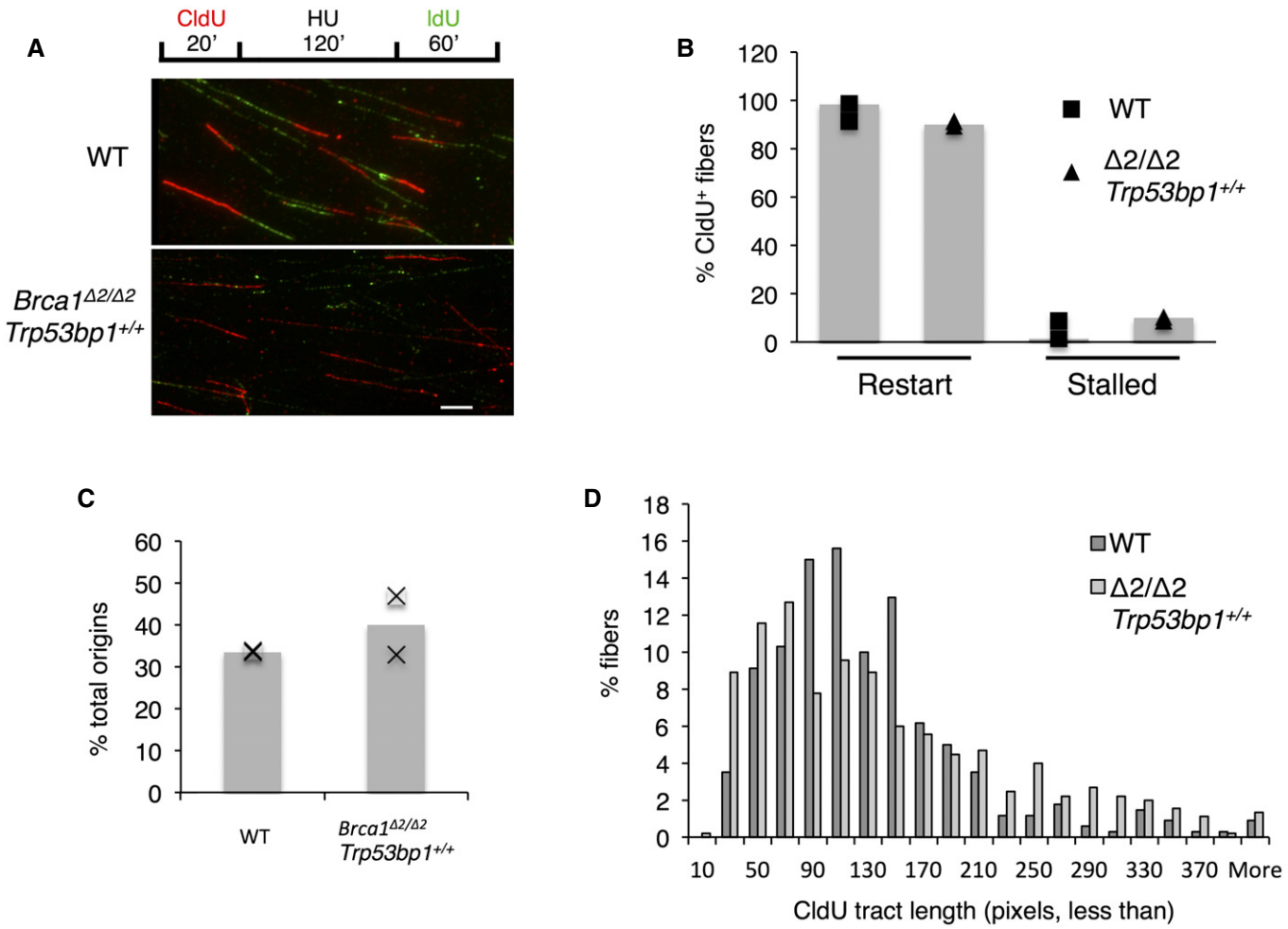

Figure 3. Replication fork stability in WT and *Brca1*$^{\Delta 2/\Delta 2}$;*Trp53bp1*$^{+/+}$ cells.

A Experimental scheme and representative images of DNA fibers. Scale bar: 5 μm.

B Analysis of fibers showing proportions of replication forks that showed restart after HU treatment or remained stalled. $N = 2$, > 500 fibers scored per experiment.

C Proportion of total forks showing *de novo* initiation after HU treatment. $N = 2$, > 500 fibers scored per experiment.

D Length of initial replication fork tracts (CldU tracts). $N = 2$, > 200 fibers measured per experiment.

[16]. To test whether *Brca1*$^{ex2/ex2}$;*Trp53bp1*$^{-/-}$ mice are susceptible to tumors, we performed a longitudinal study of cohorts of *Brca1*$^{ex2/ex2}$;*Trp53bp1*$^{-/-}$ and *Brca1*$^{ex2/+}$;*Trp53bp1*$^{-/-}$ animals (Fig 4A). The lifespan of the *Brca1*$^{ex2/ex2}$;*Trp53bp1*$^{-/-}$ mice was not significantly altered compared to *Brca1*$^{ex2/+}$;*Trp53bp1*$^{-/-}$ littermates. The frequency of tumors in *Brca1*-deficient mice is greatly increased in the absence of one or both copies of *Trp53*, which encodes the p53 tumor suppressor [24]. We therefore bred additional cohorts of *Brca1*$^{ex2/ex2}$;*Trp53bp1*$^{-/-}$;*Trp53*$^{+/-}$ and *Brca1*$^{ex2/+}$;*Trp53bp1*$^{-/-}$;*Trp53*$^{+/-}$ mice to test whether loss of p53 affected survival in mice expressing RING-less BRCA1 (Fig 4B). Although in each case the animals on a *Trp53*$^{+/-}$ background showed a decreased survival relative to the *Trp53*$^{+/+}$ cohort, there was no statistically significant difference in survival between *Brca1*$^{ex2/ex2}$;*Trp53bp1*$^{-/-}$;*Trp53*$^{+/-}$ and *Brca1*$^{ex2/+}$;*Trp53bp1*$^{-/-}$;*Trp53*$^{+/-}$ animals. A number of animals from both the *Brca1*$^{ex2/ex2}$;*Trp53bp1*$^{-/-}$ and *Brca1*$^{ex2/+}$;*Trp53bp1*$^{-/-}$ cohorts showed abnormal growth affecting one or more tissues at the time of death, but there was no increase in the frequency of abnormal tissue morphology in the *Brca1*$^{ex2/ex2}$;*Trp53bp1*$^{-/-}$ mice compared to littermate controls (Fig 4C). Abnormal growth most commonly affected the spleen, consistent with lymphoma, which has previously been reported in old *Trp53bp1*$^{-/-}$ mice (Fig 4D) [25]. Expression of RING-less BRCA1 instead of the full-length protein therefore does not cause any increase in tumor susceptibility when 53BP1 is absent.

Several phenotypes of *Brca1* deficiency were not rescued by *Trp53bp1* deletion. Hypersensitivity of *Brca1*$^{\Delta 2/\Delta 2}$ cells to cisplatin was not relieved by *Trp53bp1* deletion (Fig EV1B). This matches the phenotype of *Brca1*$^{\Delta 11/\Delta 11}$;*Trp53bp1*$^{-/-}$ cells, which are also hypersensitive to cisplatin [16]. Male *Brca1*$^{ex2/ex2}$;*Trp53bp1*$^{-/-}$ mice are also infertile, with reduced testis size [16]. To gain further insight into the requirement for BRCA1 for normal spermatogenesis, we made sections of testes from adult male *Brca1*$^{ex2/ex2}$;*Trp53bp1*$^{-/-}$ mice. H&E staining revealed that the seminiferous tubules in *Brca1*$^{ex2/ex2}$;*Trp53bp1*$^{-/-}$ mice were markedly less populated than wild-type tubules and showed no spermatids or spermatozoa

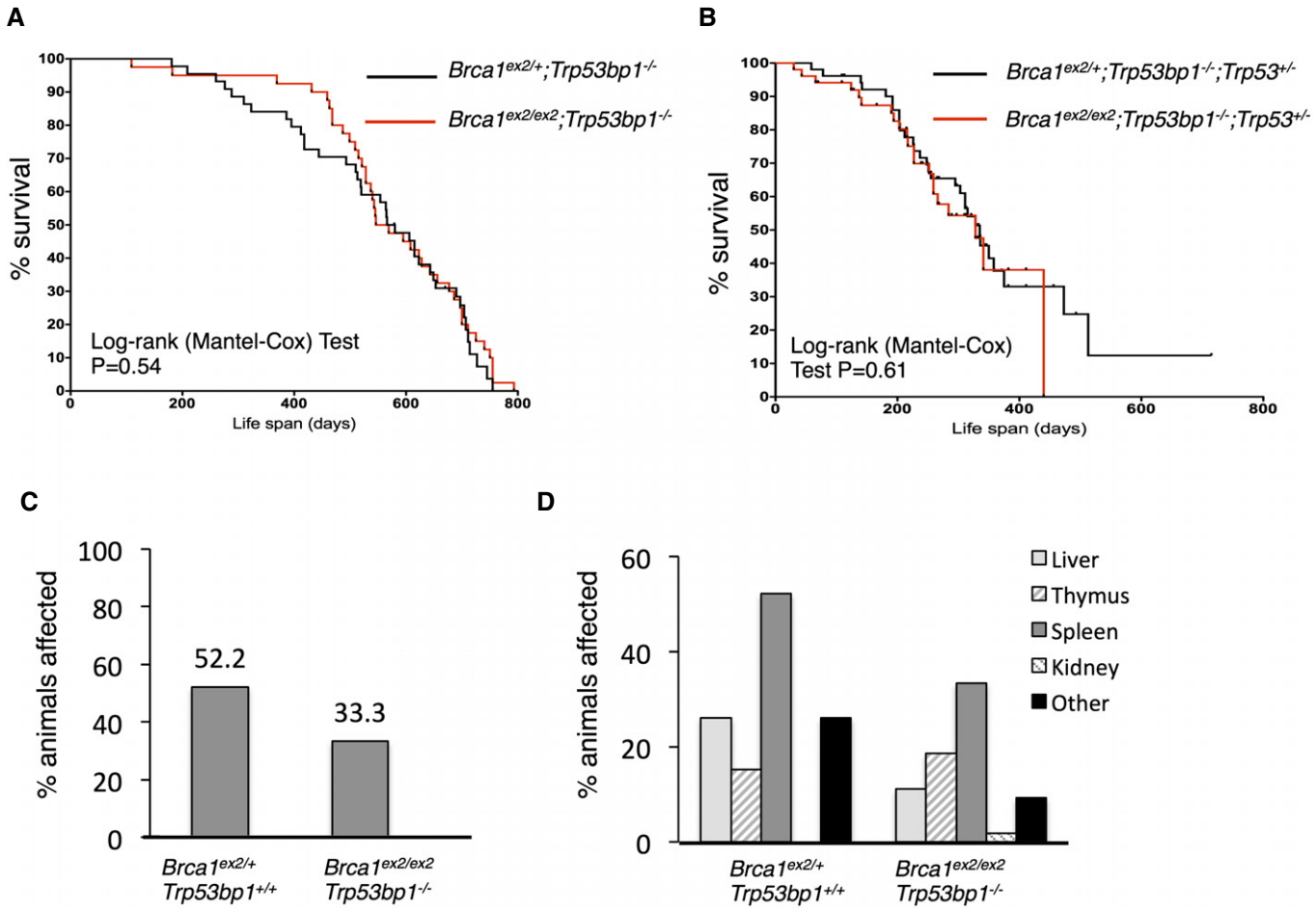

Figure 4. Lifespan and tumor predisposition of mice expressing RING-less BRCA1.

A Kaplan–Meier survival curve for *Brca1*$^{ex2/+}$;*Trp53bp1*$^{-/-}$ and *Brca1*$^{ex2/ex2}$;*Trp53bp1*$^{-/-}$ mice. $N = 20$ animals in each group. Statistical analysis by Mantel–Cox log-rank test.

B Kaplan–Meier survival curve for *Brca1*$^{ex2/+}$;*Trp53bp1*$^{-/-}$;*Trp53*$^{+/-}$ and *Brca1*$^{ex2/ex2}$;*Trp53bp1*$^{-/-}$;*Trp53*$^{+/-}$ mice. $N = 20$ animals in each group. Statistical analysis by Mantel–Cox log-rank test.

C Percentage of *Brca1*$^{ex2/+}$;*Trp53bp1*$^{-/-}$ and *Brca1*$^{ex2/ex2}$;*Trp53bp1*$^{-/-}$ mice showing signs of abnormal tissue morphology at death. $N = 46$ animals inspected for *Brca1*$^{ex2/+}$;*Trp53bp*$^{+/+}$, $N = 54$ animals inspected for *Brca1*$^{ex2/ex2}$;*Trp53bp1*$^{-/-}$.

D Tissues affected by abnormal growth from $N = 46$ *Brca1*$^{ex2/+}$;*Trp53bp1*$^{-/-}$ and $N = 54$ *Brca1*$^{ex2/ex2}$;*Trp53bp1*$^{-/-}$ mice.

(Fig 5A). The cellular density and identity within seminiferous tubules is consistent with arrest during the first meiotic prophase [26]. To determine at which stage we observe meiotic prophase arrest, we analyzed meiotic chromosome spreads from *Brca1*$^{ex2/ex2}$;*Trp53bp1*$^{-/-}$ spermatocytes. RAD51, DMC1, and γ-H2AX foci form normally in early meiotic prophase I *Brca1*$^{ex2/ex2}$;*Trp53bp1*$^{-/-}$ spermatocytes (data not shown), indicating that DSBs are formed with wild-type kinetics. Chromosome pairing is for the most part normal in *Brca1*$^{ex2/ex2}$;*Trp53bp1*$^{-/-}$ spermatocytes; however, asynapsis of one or two chromosomes is observed at a higher rate than in equivalently staged wild-type spermatocytes (56 versus 20%, $P = 0.0242$, Fisher's exact test, two-tailed). Spermatogenesis in *Brca1*$^{ex2/ex2}$;*Trp53bp1*$^{-/-}$ mice is arrested at the pachytene stage of meiosis I (Fig 5B), likely due to a failure to form an adequate sex body, the heterochromatic region that houses the sex chromosomes and results in their transcriptional repression [27]. If the sex body fails to form, sex chromosome genes are inappropriately expressed resulting in pachytene-stage apoptosis. We observed that all of the *Brca1*$^{ex2/ex2}$;*Trp53bp1*$^{-/-}$ spermatocytes formed a nascent sex body as delineated by a region of dense γ-H2AX staining overlapping the heteromorphic sex chromosomes (Fig 5B). However, the majority (87%) of *Brca1*$^{ex2/ex2}$;*Trp53bp1*$^{-/-}$ spermatocytes had a portion of the sex chromosomes, usually the centromeric region of the X chromosome, excluded from the sex body (arrow in Fig 5B). By contrast, only 7% of wild-type spermatocytes exhibited a similar exclusion of a sex chromosome at early pachynema ($P < 0.0001$, Fisher's exact test, two-tailed). Finally, ectopic γ-H2AX staining was frequently observed on the autosomes of *Brca1*$^{ex2/ex2}$;*Trp53bp1*$^{-/-}$ spermatocytes (Fig 5B and C), indicating a failure to efficiently repair meiotic DSBs. The phenotypes observed for *Brca1*$^{ex2/ex2}$;*Trp53bp1*$^{-/-}$ spermatocytes are similar to that reported previously in *Brca1*$^{\Delta 11/\Delta 11}$;*Trp53*$^{+/-}$ mice [28] and show that BRCA1 has an essential role in spermatogenesis that is independent of 53BP1. As *Trp53bp1*$^{-/-}$ mice do not show a defect in spermatogenesis, this observation suggests that the RING domain of BRCA1 is required for normal spermatogenesis.

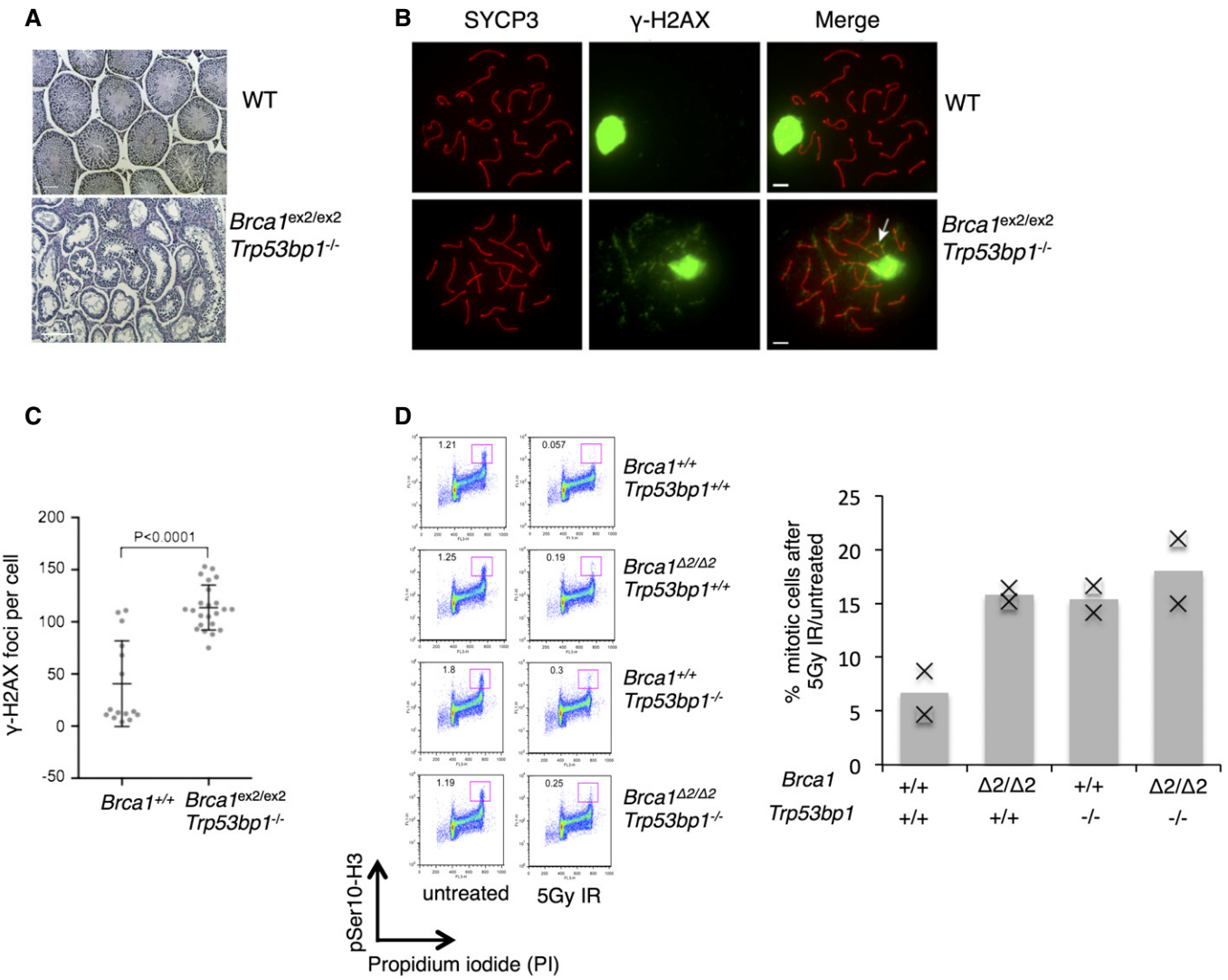

Figure 5. Arrest in spermatogenesis in mice expressing RING-less BRCA1.

A H&E-stained sections of seminiferous tubules from testes of WT and *Brca1*$^{ex2/ex2}$;*Trp53bp1*$^{-/-}$ male mice. Scale bar: 100 μm.

B Immunofluorescence on meiotic chromosomes from WT and *Brca1*$^{ex2/ex2}$;*Trp53bp1*$^{-/-}$ spermatocytes. Spreads were stained for SYCP3 to indicate chromosome axes and extent of synapsis and γ-H2AX to indicate sex body. Scale bar: 5 μm.

C Quantification of the number of γ-H2AX foci observed at the pachytene stage in the indicated genotypes. *P*-value is Mann–Whitney, two-tailed.

D G_2M checkpoint analysis in mouse B cells after IR treatment. Left, mitotic cells were identified by flow cytometry as having 4c DNA content (based on propidium iodide staining) and pSer10-H3$^+$. Right, quantification of flow cytometry data, showing mitotic cells after IR as the percentage of that seen in untreated cells. $N \geq 2$.

Cells exposed to IR induce a checkpoint at the transition between G_2 and M phase of the cell cycle, which prevents mitosis in the presence of broken chromosomes. This G_2M checkpoint is deficient in cells lacking functional BRCA1 [29]. We measured the percentage of mitotic cells after exposure to IR and observed that WT cells showed a strong induction of the G_2M checkpoint, with very few mitotic cells post-IR, whereas *Brca1*$^{\Delta 2/\Delta 2}$ cells showed a defect in checkpoint induction (Fig 5D). This defect was not rescued in *Brca1*$^{\Delta 2/\Delta 2}$;*Trp53bp1*$^{-/-}$ cells, which showed an equivalent percentage of mitotic cells after IR treatment as was seen in *Brca1*$^{\Delta 2/\Delta 2}$;*Trp53bp1*$^{+/+}$ cells. Deletion of *Trp53bp1* therefore does not cause a measurable rescue of the G_2M checkpoint defect of *Brca1*-deficient cells, although the deletion of *Trp53bp1* is by itself sufficient to cause a G_2M checkpoint defect [30].

Taken together, our results suggest a more complex picture for how BRCA1 and 53BP1 collaborate to maintain the genomic integrity. Our previous work demonstrated that the deletion of *Trp53bp1* rescues embryonic lethality and tumor predisposition of *Brca1*$^{\Delta 11/\Delta 11}$ mice by promoting the resection of DSBs, thereby facilitating homologous recombination [10,12]. Notably, the deletion of *Trp53bp1* correlated with rescue of RAD51 foci formation after ionizing radiation, a hallmark of homologous recombination that is normally deficient in *Brca1*$^{\Delta 11/\Delta 11}$ cells. Our findings with *Brca1*$^{\Delta 2/\Delta 2}$ cells suggest that 53BP1 has an effect in regulating genomic integrity that is separable from RAD51 foci formation.

Brca1$^{\Delta 2/\Delta 2}$ cells are capable of forming RAD51 foci, but still show genomic instability when 53BP1 is present. The defect in genomic maintenance in cells expressing RING-less BRCA1 appears to arise during replication, suggesting that 53BP1 is also active in the control of replication fork restart. It is not clear how the RING domain of BRCA1 mediates replication fork restart. In complex with BARD1, the BRCA1 RING domain acts as an E3 ubiquitin ligase [4], which may be relevant for overcoming replication barriers or removing covalent adducts that compromise replication fork progression. On the other hand, *Brca1*$^{I26A/I26A}$ mice, which express enzymatically deficient BRCA1, are viable and show no significant genomic instability [8,9].

RING-less BRCA1 has several features in common with the mutant protein expressed in *Brca1*$^{C61G/C61G}$ mice, which are a model for the common *BRCA1*-C61G patient mutation [31]. The C61G mutation destabilizes the BRCA1 RING domain and prevents association with BARD1. As is the case with RING-less BRCA1, BRCA1^{C61G} protein is unable to maintain genomic integrity or act as a tumor suppressor, but BRCA1^{C61G} protein can nonetheless contribute to chemoresistance of tumor cells. The ability of N-terminal truncated isoforms of BRCA1 to partially support repair activity is of potential clinical significance. The common *BRCA1* founder mutation 185delAG is a deletion of two nucleotides, which creates a premature stop codon in exon 3 and prevents the expression of full-length BRCA1 protein. In 185delAG patient cells, BRCA1 protein expression could hypothetically be reinitiated from a downstream start codon, resulting in production of a RING-less BRCA1 isoform, similar to that observed in *Brca1*$^{\Delta 2/\Delta 2}$ cells. Any such N-terminal-deleted BRCA1 isoforms could contribute to tumor progression or chemoresistance by facilitating a subset of DNA repair activities, especially in cells lacking 53BP1. Two recent reports have supported the idea that the expression of BRCA1^{185delAG} can contribute to tumor chemoresistance in mouse models and human cancer cell lines [32,33]. Our results also show that the ability to form RAD51 foci may not be a reliable indicator for BRCA1 tumor suppressor activity, as mutant BRCA1 isoforms may support RAD51 foci formation, while still being unable to maintain genomic integrity.

Materials and Methods

Mice

Brca1$^{ex2/+}$ mice [13] were crossed with *Trp53bp1*$^{-/-}$ mice [34]. *Brca1*$^{flex2/+}$ mice [14] were additionally crossed to *Trp53bp1*$^{-/-}$ mice and CD19-Cre mice [34]. *Brca1*$^{\Delta 11/\Delta 11}$;*Trp53bp1*$^{-/-}$ mice were as described [12]. All animals were housed in sterile conditions under a protocol approved by the Rutgers University Institute Animal Care and Use Committee.

Immunofluorescence

For immunofluorescence of mouse embryonic fibroblasts (MEFs), cells were grown on sterile coverslips overnight. For B-cell immunofluorescence, cells were applied to slides coated with CellTak (Corning). Radiation treatment to induce DSBs was 10 Gy ionizing radiation from a ^{137}Cs source followed by 4-h recovery at 37°C. Fixation was carried out with 2% paraformaldehyde followed by the treatment with 0.5% Triton X-100. Antibodies used were mouse monoclonal α-BRCA1 (aa160-300) [36]; rabbit polyclonal α-RAD51 (Santa Cruz); rabbit polyclonal α-BARD1 [6]. Fixed stained nuclei were counterstained with DAPI and imaged using a Nikon Eclipse E800 epifluorescence microscope.

Mass spectrometry

Protein lysates from activated WT and *Brca1*$^{\Delta 2/\Delta 2}$;*Trp53bp1*$^{-/-}$ mouse B cells (200 μg protein each) were separated by SDS–PAGE. For each, the region predicted to contain the protein of interest (~200 kD) was excised and digested with trypsin. Digests were analyzed using a Q Exactive HF tandem mass spectrometer coupled to a Dionex Ultimate 3000 RLSCnano System (Thermo Scientific). Samples were solubilized in 5% acetonitrile/0.1% TFA and loaded on to a fused silica trap column of 100 μm × 2 cm packed with Magic C18AQ, 5 μm 200+ (Michrom Bioresources Inc, Auburn, CA). After washing for 5 min at 10 μl/min with solvent A (0.2% formic acid), the flow rate was reduced to 300 nl/min and the trap brought in-line with a homemade analytical column (Magic C18AQ, 3 μm 200 A, 75 μm × 50 cm) for LC-MS/MS. Peptides were eluted using a segmented linear gradient from 4 to 90% solvent B (B: 0.08% formic acid, 80% ACN): 4% B for 5 min, 4–15% B for 19 min, 15–25% B for 40 min, 25–50% B for 55 min, and 50–90% B for 8 min. Mass spectrometry data were acquired using parallel reaction monitoring targeting previously observed BRCA1_mouse tryptic peptides in the region of interest found in GPMdb (http://gpmdb.thegpm.org/) [37] as well as the potential alternative start sites for the mutant. Instrument settings were as follows: resolution 30,000 (at m/z 200); AGC target 5E5; maximum fill time 100 ms; precursor isolation window 1.4 m/z; and normalized collision energy of 25 for fragmentation. The raw files were analyzed using Xcalibur Qual browser (Thermo Fisher).

Spermatocyte chromosome spreads and immunofluorescence

Spermatocytes from mice between 2 and 6 months of age were individualized in suspension, surface-spread, and stained for immunofluorescence as previously described [38]. Identity and concentrations of antibodies used were as follows: SYCP3 (Abcam ab15093 at 1:500 and Santa Cruz sc-74569 at 1:500); RAD51 (Calbiochem PC130 at 1:200); γ-H2AX (Millipore JBW301, 1:10,000); MLH1 (Pharmingen 551092, 1:50). Spreads from at least two mice of each genotype were analyzed.

Preparation and hybridization of chromosome spreads

Resting B lymphocytes were isolated from mouse spleens and cultured with LPS (25 μg/ml, Sigma) and IL-4 (5 ng/ml, Sigma) as described [12]. After 36-h growth, the cells were mock-treated or treated with olaparib (2 μM) overnight, then arrested with 10 μg/ml colcemid for 1 h. Metaphase fixation and telomere PNA-FISH was performed as previously described [39].

DNA combing

Splenic B cells were grown *in vitro* for 48 h. The cells were pulsed with CldU, HU, and IdU, and the fibers were prepared, stained, and analyzed as previously described [40].

G_2M checkpoint analysis

The activated B cells were exposed to 5 Gy ionizing radiation, allowed to recover for 1 h, and then fixed with cold 70% ethanol. Staining of mitotic cells was achieved using rabbit polyclonal α-phospho-H3 antibody (Millipore). Cellular DNA was stained with 10 μg/ml propidium iodide, and flow cytometry data were acquired on a FACS Calibur instrument using CellQuest.

Statistics

Survival curves were plotted using the Kaplan–Meier method, and the Mantel–Cox log-rank test was used to evaluate the statistical differences between cohorts in the mouse aging study. Other experimental outcomes were analyzed using a two-tailed Student's *t*-test. A *P*-value of < 0.05 was considered to be statistically significant.

Study approval

All animal experiments were conducted under an animal protocol approved by the IACUC of Rutgers University.

Expanded View for this article is available online.

Acknowledgements
Thanks to Dr. Peter Lobel for advice on MS and Jake Altshuler for assistance with data analysis. This work was supported by NCI R00CA160574. DP and SM were supported by the Rutgers Biotech Training Program (T32 GM008339) and by predoctoral awards from the New Jersey Commission on Cancer Research. FC was supported by NIH grant DP2HD087943. The Rutgers Biological Mass Spectrometry Facility was supported by NIH S10OD016400.

Author contributions
ML performed most experiments directed by SFB, who wrote the manuscript. FC did analysis of meiosis and assisted with the manuscript. DSP did RAD51 IF. SMM prepared the samples for MS and SCE analysis. JH performed additional IF experiments. AM maintained mouse cohorts and prepared the samples for the tumorigenesis study. AA performed RT–PCR analysis of *Brca1* expression. HZ conducted MS experiments. RB, TL, MJ, and AN assisted with writing of the manuscript. LS designed and conducted the DNA combing experiments.

Conflict of interest
The authors declare that they have no conflict of interest.

References

1. Brodie SG, Deng CX (2001) BRCA1-associated tumorigenesis: what have we learned from knockout mice? *Trends Genet* 17: S18 – S22
2. Roy R, Chun J, Powell SN (2012) BRCA1 and BRCA2: different roles in a common pathway of genome protection. *Nat Rev Cancer* 12: 68 – 78
3. Moynahan ME, Chiu JW, Koller BH, Jasin M (1999) Brca1 controls homology-directed DNA repair. *Mol Cell* 4: 511 – 518
4. Hashizume R, Fukuda M, Maeda I, Nishikawa H, Oyake D, Yabuki Y, Ogata H, Ohta T (2001) The RING heterodimer BRCA1-BARD1 is a ubiquitin ligase inactivated by a breast cancer-derived mutation. *J Biol Chem* 276: 14537 – 14540
5. Kalb R, Mallery DL, Larkin C, Huang JT, Hiom K (2014) BRCA1 is a histone-H2A-specific ubiquitin ligase. *Cell Rep* 8: 999 – 1005
6. Wu LC, Wang ZW, Tsan JT, Spillman MA, Phung A, Xu XL, Yang MC, Hwang LY, Bowcock AM, Baer R (1996) Identification of a RING protein that can interact in vivo with the BRCA1 gene product. *Nat Genet* 14: 430 – 440
7. Zhu Q, Pao GM, Huynh AM, Suh H, Tonnu N, Nederlof PM, Gage FH, Verma IM (2011) BRCA1 tumour suppression occurs via heterochromatin-mediated silencing. *Nature* 477: 179 – 184
8. Reid LJ, Shakya R, Modi AP, Lokshin M, Cheng JT, Jasin M, Baer R, Ludwig T (2008) E3 ligase activity of BRCA1 is not essential for mammalian cell viability or homology-directed repair of double-strand DNA breaks. *Proc Natl Acad Sci USA* 105: 20876 – 20881
9. Shakya R, Reid LJ, Reczek CR, Cole F, Egli D, Lin CS, deRooij DG, Hirsch S, Ravi K, Hicks JB *et al* (2011) BRCA1 tumor suppression depends on BRCT phosphoprotein binding, but not its E3 ligase activity. *Science* 334: 525 – 528
10. Cao L, Xu X, Bunting SF, Liu J, Wang RH, Cao LL, Wu JJ, Peng TN, Chen J, Nussenzweig A *et al* (2009) A selective requirement for 53BP1 in the biological response to genomic instability induced by Brca1 deficiency. *Mol Cell* 35: 534 – 541
11. Bouwman P, Aly A, Escandell JM, Pieterse M, Bartkova J, van der Gulden H, Hiddingh S, Thanasoula M, Kulkarni A, Yang Q *et al* (2010) 53BP1 loss rescues BRCA1 deficiency and is associated with triple-negative and BRCA-mutated breast cancers. *Nat Struct Mol Biol* 17: 688 – 695
12. Bunting SF, Callen E, Wong N, Chen HT, Polato F, Gunn A, Bothmer A, Feldhahn N, Fernandez-Capetillo O, Cao L *et al* (2010) 53BP1 inhibits homologous recombination in Brca1-deficient cells by blocking resection of DNA breaks. *Cell* 141: 243 – 254
13. Ludwig T, Chapman DL, Papaioannou VE, Efstratiadis A (1997) Targeted mutations of breast cancer susceptibility gene homologs in mice: lethal phenotypes of Brca1, Brca2, Brca1/Brca2, Brca1/p53, and Brca2/p53 nullizygous embryos. *Genes Dev* 11: 1226 – 1241
14. Shakya R, Szabolcs M, McCarthy E, Ospina E, Basso K, Nandula S, Murty V, Baer R, Ludwig T (2008) The basal-like mammary carcinomas induced by Brca1 or Bard1 inactivation implicate the BRCA1/BARD1 heterodimer in tumor suppression. *Proc Natl Acad Sci USA* 105: 7040 – 7045
15. Evers B, Jonkers J (2006) Mouse models of BRCA1 and BRCA2 deficiency: past lessons, current understanding and future prospects. *Oncogene* 25: 5885 – 5897
16. Bunting SF, Callen E, Kozak ML, Kim JM, Wong N, Lopez-Contreras AJ, Ludwig T, Baer R, Faryabi RB, Malhowski A *et al* (2012) BRCA1 functions independently of homologous recombination in DNA interstrand cross-link repair. *Mol Cell* 46: 125 – 135
17. Brzovic PS, Keeffe JR, Nishikawa H, Miyamoto K, Fox D 3rd, Fukuda M, Ohta T, Klevit R (2003) Binding and recognition in the assembly of an active BRCA1/BARD1 ubiquitin-ligase complex. *Proc Natl Acad Sci USA* 100: 5646 – 5651
18. Joukov V, Chen J, Fox EA, Green JB, Livingston DM (2001) Functional communication between endogenous BRCA1 and its partner, BARD1, during Xenopus laevis development. *Proc Natl Acad Sci USA* 98: 12078 – 12083
19. Lu Y, Amleh A, Sun J, Jin X, McCullough SD, Baer R, Ren D, Li R, Hu Y (2007) Ubiquitination and proteasome-mediated degradation of BRCA1 and BARD1 during steroidogenesis in human ovarian granulosa cells. *Mol Endocrinol* 21: 651 – 663
20. Prakash R, Zhang Y, Feng W, Jasin M (2015) Homologous recombination and human health: the roles of BRCA1, BRCA2, and associated proteins. *Cold Spring Harb Perspect Biol* 7: a016600

21. Sy SM, Huen MS, Chen J (2009) PALB2 is an integral component of the BRCA complex required for homologous recombination repair. *Proc Natl Acad Sci USA* 106: 7155 – 7160
22. Schlacher K, Wu H, Jasin M (2012) A distinct replication fork protection pathway connects Fanconi anemia tumor suppressors to RAD51-BRCA1/2. *Cancer Cell* 22: 106 – 116
23. Ray Chaudhuri A, Callen E, Ding X, Gogola E, Duarte AA, Lee JE, Wong N, Lafarga V, Calvo JA, Panzarino NJ *et al* (2016) Replication fork stability confers chemoresistance in BRCA-deficient cells. *Nature* 535: 382 – 387
24. Xu X, Qiao W, Linke SP, Cao L, Li WM, Furth PA, Harris CC, Deng CX (2001) Genetic interactions between tumor suppressors Brca1 and p53 in apoptosis, cell cycle and tumorigenesis. *Nat Genet* 28: 266 – 271
25. Ward IM, Minn K, van Deursen J, Chen J (2003) p53 Binding protein 53BP1 is required for DNA damage responses and tumor suppression in mice. *Mol Cell Biol* 23: 2556 – 2563
26. Meistrich ML, Hess RA (2013) Assessment of spermatogenesis through staging of seminiferous tubules. *Methods Mol Biol* 927: 299 – 307
27. Turner JM (2015) Meiotic Silencing in Mammals. *Annu Rev Genet* 49: 395 – 412
28. Turner JM, Aprelikova O, Xu X, Wang R, Kim S, Chandramouli GV, Barrett JC, Burgoyne PS, Deng CX (2004) BRCA1, histone H2AX phosphorylation, and male meiotic sex chromosome inactivation. *Curr Biol* 14: 2135 – 2142
29. Xu X, Weaver Z, Linke SP, Li C, Gotay J, Wang XW, Harris CC, Ried T, Deng CX (1999) Centrosome amplification and a defective G2-M cell cycle checkpoint induce genetic instability in BRCA1 exon 11 isoform-deficient cells. *Mol Cell* 3: 389 – 395
30. Fernandez-Capetillo O, Chen HT, Celeste A, Ward I, Romanienko PJ, Morales JC, Naka K, Xia Z, Camerini-Otero RD, Motoyama N *et al* (2002) DNA damage-induced G2-M checkpoint activation by histone H2AX and 53BP1. *Nat Cell Biol* 4: 993 – 997
31. Drost R, Bouwman P, Rottenberg S, Boon U, Schut E, Klarenbeek S, Klijn C, van der Heijden I, van der Gulden H, Wientjens E *et al* (2011) BRCA1 RING function is essential for tumor suppression but dispensable for therapy resistance. *Cancer Cell* 20: 797 – 809
32. Drost R, Dhillon KK, van der Gulden H, van der Heijden I, Brandsma I, Cruz C, Chondronasiou D, Castroviejo-Bermejo M, Boon U, Schut E *et al* (2016) BRCA1185delAG tumors may acquire therapy resistance through expression of RING-less BRCA1. *J Clin Investig* 126: 2903 – 2918
33. Wang Y, Krais JJ, Bernhardy AJ, Nicolas E, Cai KQ, Harrell MI, Kim HH, George E, Swisher EM, Simpkins F *et al* (2016) RING domain-deficient BRCA1 promotes PARP inhibitor and platinum resistance. *J Clin Investig* 126: 3145 – 3157
34. Ward IM, Reina-San-Martin B, Olaru A, Minn K, Tamada K, Lau JS, Cascalho M, Chen L, Nussenzweig A, Livak F *et al* (2004) 53BP1 is required for class switch recombination. *J Cell Biol* 165: 459 – 464
35. Rickert RC, Roes J, Rajewsky K (1997) B lymphocyte-specific, Cre-mediated mutagenesis in mice. *Nucleic Acids Res* 25: 1317 – 1318
36. Barlow JH, Faryabi RB, Callen E, Wong N, Malhowski A, Chen HT, Gutierrez-Cruz G, Sun HW, McKinnon P, Wright G *et al* (2013) Identification of early replicating fragile sites that contribute to genome instability. *Cell* 152: 620 – 632
37. Craig R, Cortens JP, Beavis RC (2004) Open source system for analyzing, validating, and storing protein identification data. *J Proteome Res* 3: 1234 – 1242
38. Cole F, Kauppi L, Lange J, Roig I, Wang R, Keeney S, Jasin M (2012) Homeostatic control of recombination is implemented progressively in mouse meiosis. *Nat Cell Biol* 14: 424 – 430
39. Misenko SM, Bunting SF (2014) Rapid analysis of chromosome aberrations in mouse B lymphocytes by PNA-FISH. *J Vis Exp* 90: e51806
40. Vazquez BN, Thackray JK, Simonet NG, Kane-Goldsmith N, Martinez-Redondo P, Nguyen T, Bunting S, Vaquero A, Tischfield JA, Serrano L (2016) SIRT7 promotes genome integrity and modulates non-homologous end joining DNA repair. *EMBO J* 35: 1488 – 1503